

Universality classes of absorbing phase transitions in generic branching-annihilating particle systems with nearest-neighbor bias

Bijoy Daga^{1,*} and Purusattam Ray^{1,2,†}

¹*The Institute of Mathematical Sciences, C.I.T Campus, Taramani, Chennai-600113, India*

²*Homi Bhabha National Institute, Training School Complex, Anushakti Nagar, Mumbai-400094, India*



(Received 16 January 2019; revised manuscript received 19 February 2019; published 5 March 2019)

We study absorbing phase transitions in systems of branching annihilating random walkers and pair contact process with diffusion on a one-dimensional ring, where the walkers hop to their nearest neighbor with a bias ϵ . For $\epsilon = 0$, three universality classes—directed percolation (DP), parity-conserving (PC), and pair contact process with diffusion (PCPD)—are typically observed in such systems. We find that the introduction of ϵ does not change the DP universality class but alters the other two universality classes. For nonzero ϵ , the PCPD class crosses over to DP, and the PC class changes to a new universality class.

DOI: [10.1103/PhysRevE.99.032104](https://doi.org/10.1103/PhysRevE.99.032104)

I. INTRODUCTION

Many reaction-diffusion systems show a second-order phase transition from a fluctuating active state to a nonfluctuating absorbing state as some control parameter is tuned [1–4]. A wide range of models corresponding to phenomena such as epidemic spreading [5], catalytic chemical reactions [6], transport in disordered media [7], forest fires [8], biological evolution [9], surface roughening [10,11], and self-activated biological structures [12] show absorbing phase transitions. These transitions are classic examples of nonequilibrium phase transitions. Studying the critical behavior and universality classes of such transitions is extremely important from a theoretical perspective and for understanding the phase transition in reaction diffusion systems.

A large number of absorbing phase transitions in nonequilibrium systems have been observed to belong to the directed percolation (DP) universality class. It has been conjectured by Janssen and Grassberger [13] that continuous absorbing phase transitions in a reaction-diffusion system with short-range interactions, characterized by a non-negative scalar order parameter and with no additional symmetries, conservation laws, and quenched randomness, belong generically to the DP universality class. The robustness of the DP universality class has been a matter of great interest among researchers. The parity-conserving (PC) universality class [14], the universality class of pair contact process with diffusion [15], the voter universality class [16], and the Manna universality class in sandpile models [17] are some noteworthy universality classes in nonequilibrium phase transitions whose critical behavior is different from that of DP.

In this work, we have focused on branching annihilating random walks (BARWs) and pair contact process with diffusion (PCPD), where three universality classes, namely, DP, PC, and PCPD, have been reported. In BARW a diffusing

random walker A can branch to produce m ($m > 0$) new off-springs $A \rightarrow (m + 1)A$, or two of them annihilate ($2A \rightarrow \emptyset$) upon meeting at the same site. The parity of the system, which is defined as the total number of walkers modulo 2, is not conserved when m is odd. Depending upon parity, the critical behavior in such systems is DP when m is odd and PC when m is even [14]. The PC class is also referred to as a directed Ising (DI) class because PC critical behavior can also be realized in spin systems when a spin-flip Glauber dynamics competes with spin-exchange Kawasaki dynamics [18]. In PCPD [15], two diffusing walkers in contact only can produce new off-springs ($2A \rightarrow 3A$) or they can annihilate ($2A \rightarrow \emptyset$). Unlike in PC, parity does not affect the critical behavior in PCPD [19].

The crossover behavior between these universality classes has been extensively studied. It has been found that the PC class crosses over to DP by introducing a dynamics which breaks the modulo 2 conservation. This is done by producing both an even and odd number of off-springs while branching [20]. In addition to PCPD dynamics, if unary branching and annihilation are introduced, then PCPD crosses over to DP when the unary process does not conserve parity [21,22] or to PC if it conserves parity [22]. This suggests that parity and n -arity of the branching process plays a crucial role in determining the universality class of the transition. It is also found that diffusion, or its absence, affects the critical behavior in a major way. For example, in the absence of diffusion, parity-conserving BARW models having spatially asymmetric branching can have additional conservation laws depending upon the initial conditions, and consequently, the decay exponent varies from the PC exponent [10]. The PCPD class crosses over continuously to DP when solitary diffusing walkers are annihilated upon contact with a certain probability which determines the value of the critical exponents [23]. When diffusion of single walkers is completely forbidden in PCPD, although the system has multiple absorbing states, its critical behavior switches over to DP [24,25]. BARW has also been studied with Ley walkers. The additional long-range correlations that build up in the system due to long-range

*bijoydaga@imsc.res.in

†ray@imsc.res.in

interactions via Ley flights lead to continuous variation of critical exponents for both DP and PC universality classes [26,27]. The above mentioned perturbations either change the parity, bring in additional conservation laws or long-range interactions, or arrest the diffusion dynamics. The effect of drive on the critical behavior of BARW and PCPD has been studied, where all the walkers diffuse in a preferential direction [28]. The driven PCPD shows a different critical behavior from the ordinary PCPD, but DP and PC critical behaviors remain unchanged under such a drift.

We ask what happens to DP, PC, and PCPD universal critical behaviors when only local perturbations are introduced to the underlying diffusion dynamics without affecting parity of the system, creating any long-range interactions, or bringing in additional conservation laws. Specifically, we study BARW and PCPD on a one-dimensional periodic chain where the walkers hop to their nearest neighbor with a bias ϵ . A walker at a given site diffuses towards its nearest neighbor with probability $\frac{1}{2} + \epsilon$ ($0 \leq \epsilon \leq 1/2$) and in the opposite direction with the complimentary probability $\frac{1}{2} - \epsilon$. For $\epsilon = 0$, the walker performs a simple random walk, and for $\epsilon = 1/2$, the walker moves ballistically towards its nearest neighbor. It is to be noted that the bias on a walker at different sites is uncorrelated as is the bias on the walker at different times, and therefore there is no net drive on the system. The process retains its Markovian nature, and unlike the problem with a Ley walker, there is no additional long-range interaction that is present in the system. However, the bias hinders the diffusion of walkers away from their parent cluster. Thus, for $\epsilon > 0$, branching and annihilation within a cluster become the dominant processes. The case of annihilating random walkers (i.e., no branching) in presence of the bias ϵ has been studied [29], and it was found that the decay exponent changes from a value $1/2$ without bias to 1 when bias is introduced. This suggests that under the bias, the random walkers at large times behave as ballistic walkers. When branching is turned on, there is an absorbing phase transition for $\epsilon = 0$ [14,15]. With $\epsilon > 0$, one would expect the transition between absorbing and active phases to occur at higher branching rates because of the enhanced annihilation.

An important question to ask is whether this bias will affect the critical behavior of the transition and what are the possible universality classes it can give rise to. We study the problem using Monte Carlo simulations. We find that nonzero ϵ retains the universality class of DP, whereas the PCPD class changes to DP and the PC class changes to a new universality class.

II. MODELS

On a one-dimensional lattice, the BARW with nearest-neighbor bias ϵ ($0 \leq \epsilon \leq 1/2$) is defined in the following way: with probability p , a random walker A diffuses, and with the complimentary probability $1 - p$ it branches to produce m ($m > 0$) off-springs: $A \rightarrow (m + 1)A$ at its nearest-neighbor sites. When a walker diffuses, it does so with a probability $\frac{1}{2} + \epsilon$ towards its nearest-neighbor walker and with probability $\frac{1}{2} - \epsilon$ in the opposite direction. When two walkers meet at the same site, they annihilate ($2A \rightarrow \emptyset$). For large values of p , all walkers get annihilated, and the system goes to an absorbed state. When p is small, the branching rate

being higher, the system has a finite density of walkers even at large times, and hence the system remains active forever. Therefore, by varying p , one can observe absorbing phase transitions in such systems at a particular critical value of $p = p_c$. When m is even, the number of walkers modulo 2 is conserved at all times. This symmetry is called the parity. For $\epsilon = 0$, the critical behavior of the transition between active and absorbing states depends upon parity. The critical behavior in these systems belongs to PC when m is even and to DP when m is odd [14]. We vary ϵ and determine how the critical behavior of the absorbing phase transitions change for the $m = 1$ and $m = 4$ cases. For the case of parity-conserving BARW, we choose $m = 4$ instead of $m = 2$, because on a one-dimensional lattice, p_c is trivially equal to zero for $m = 2$ [14].

We also study the effect of the nearest-neighbor bias on a binary process like PCPD [15], where branching can occur only when two random walkers are placed side by side. A walker is selected at random, and its neighboring site (left or right) is chosen with equal probability. The system then evolves by following one of the three processes with the respective assigned probabilities:

(1) With probability $q(1 - D)$, the walker and its neighbor in the chosen site are annihilated ($2A \rightarrow \emptyset$).

(2) If the chosen neighboring site is occupied and the next nearest site in the direction of the neighboring site is empty, a new walker is created ($2A \rightarrow 3A$) at the next nearest site with probability $(1 - q)(1 - D)$.

(3) A walker diffuses with probability D to one of its neighboring site (left or right) if it is empty. In this step the neighboring site is not chosen with equal probability. The target site for the diffusing walker is chosen with probability $1/2 + \epsilon$ towards its nearest-neighbor walker and with probability $1/2 - \epsilon$ in the opposite direction.

For $\epsilon = 0$, the critical point and the critical exponents for absorbing phase transition in PCPD generally depends upon both q and D [15]. In this work, we find the critical point q_c for a fixed value of $D = 1/2$ and study how the critical behavior changes as ϵ is varied.

III. SIMULATION

To simulate BARW and PCPD, we start with a fully occupied lattice at time $t = 0$ and measure the average density of walkers $\rho(t) = \langle s_i(t) \rangle$ as a function of time. Here the $\langle \dots \rangle$ represents the average over configurations. The variable $s_i(t)$ takes the value 1 when site i is occupied by a walker and 0 when it is unoccupied. As $t \rightarrow \infty$, $\rho(t)$ saturates to a positive value ρ_a , if the system is in the active phase ($p < p_c$ or $q < q_c$) and decays to zero in the absorbing phase ($p > p_c$ or $q > q_c$). Thus, effectively, $\rho(t)$ acts as an order parameter for the system. At the critical point where $p = p_c$ for BARW and $q = q_c$ for PCPD, density decays with time as a power law,

$$\rho(t) \sim t^{-\alpha}, \quad (1)$$

α being the decay exponent. The critical points p_c , q_c , and the decay exponent α can be estimated by plotting $\rho(t)$ versus t for different values of p and q , respectively. At the critical point, a power law is obtained. For illustration, in Figs. 1 and 2 we make an estimate of

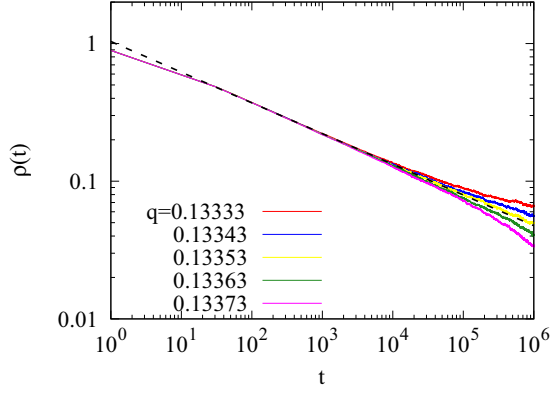


FIG. 1. Log-log plot of $\rho(t)$ vs t when $\epsilon = 0$ in the PCPD model for various values of q , where the value of q increases as one moves from top to bottom of the panel. For $q = 0.13353$, the density decays with a power law as shown by the dashed line, thus giving an estimate of the critical point $q_c = 0.13353$. The slope of the dashed line gives the estimate of the decay exponent $\alpha \sim 0.221$. Here $L = 25\,000$.

the critical point q_c and the exponent α in the PCPD model for $\epsilon = 0$ and $\epsilon = 1/2$, respectively. We also show the estimated value of α in BARW ($m = 4$) for $\epsilon = 0$, $1/2$ in Fig. 3. For different values of ϵ , the estimate of the critical point and α for BARW and PCPD has been compiled in Table I.

The dynamical exponent z can be determined from the finite-size scaling analysis. In a finite system of size L , the decay of $\rho(t)$ as a function of t at the critical point has the scaling form

$$\rho(t, L) \sim t^{-\alpha} f(t/L^z), \quad (2)$$

where f is a scaling function. $f(x)$ is a constant for $x \ll 1$ and decays exponentially for larger values of x . Once α has been measured, one can then determine z using Eq. (2). At the critical point, the curves $\rho(t)t^\alpha$ versus t/L^z for different values of L collapse to a single curve. In Figs. 4, 5, 6, and 7, we use

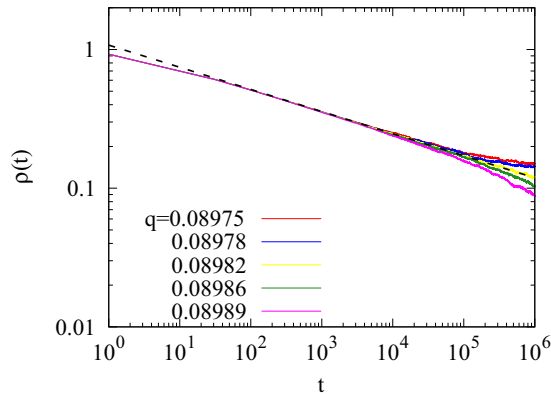


FIG. 2. Log-log plot of $\rho(t)$ vs t when $\epsilon = 1/2$ in PCPD model for different values of q , where the value of q increases as one moves from top to bottom of the panel. For $q = 0.08982$, the density decays with a power law as shown by the dashed line, thus giving an estimate of the critical point $q_c = 0.08982$. The slope of the dashed line gives the estimate of the decay exponent $\alpha \sim 0.159$. Here $L = 25\,000$.

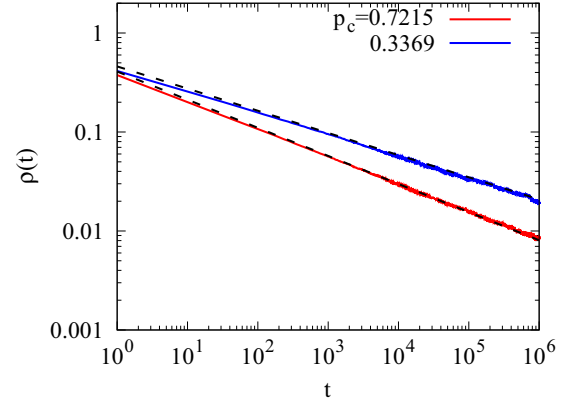


FIG. 3. Log-log plot of $\rho(t)$ vs t in BARW ($m = 4$) model at the estimated critical points $p_c = 0.7215$ for $\epsilon = 0$ (lower line in the panel) and $p_c = 0.3369$ for $\epsilon = 1/2$ (upper line), respectively. The density decays with a power law as shown by the dashed lines. The slope of the dashed line gives the estimate of the decay exponent $\alpha \sim 0.284$ for $\epsilon = 0$, and $\alpha \sim 0.224$ for $\epsilon = 1/2$.

the finite-size scaling method to measure z for BARW ($m = 4$) and PCPD when $\epsilon = 0$ and $\epsilon = 1/2$. For BARW ($m = 4$), the data for different values of L collapse when $z = 1.75$ for $\epsilon = 0$ and $z = 1.74$ for $\epsilon = 1/2$. For PCPD, a good data collapse is obtained when $z = 1.72$ for $\epsilon = 0$ and $z = 1.59$ for $\epsilon = 1/2$.

The order parameter exponent β characterizes the algebraic decay of the density ρ_a as one approaches the critical point p_c ($p \rightarrow p_c^-$ for BARW) or q_c ($q \rightarrow q_c^-$ for PCPD) in the active phase:

$$\rho_a \sim (p_c - p)^\beta \text{ and } \rho_a \sim (q_c - q)^\beta. \quad (3)$$

Figures 8 and 9 shows the logarithmic plot of ρ_a versus $p_c - p$ for BARW ($m = 4$) and ρ_a versus $q_c - q$ for PCPD and estimated values of β for $\epsilon = 0$ and $\epsilon = 1/2$.

TABLE I. Numerical estimate of critical points and critical exponents in BARW and PCPD for various values of ϵ obtained using Monte Carlo simulations. The numbers within parentheses represent the error in the last decimal place. The errors are determined from an eye estimate in fitting the exponents in the power laws and the scaling function.

Model	ϵ	p_c	α	β	z	θ
BARW $m = 1$	0	0.1070(1)	0.161(1)	0.278(1)	1.58(1)	0.251(1)
	0.1	0.08355(3)	0.159(2)	0.276(1)	1.59(1)	0.250(1)
	0.3	0.05819(4)	0.159(2)	0.275(2)	1.58(1)	0.251(2)
	0.5	0.04469(2)	0.158(1)	0.276(1)	1.58(1)	0.250(2)
BARW $m = 4$	0	0.7215(5)	0.284(3)	0.92(4)	1.75(1)	0.491(2)
	0.1	0.5620(2)	0.232(4)	0.55(1)	1.72(1)	0.381(5)
	0.3	0.4182(2)	0.229(3)	0.53(1)	1.71(2)	0.378(3)
	0.5	0.3369(2)	0.224(5)	0.51(2)	1.74(2)	0.376(2)
PCPD	ϵ	q_c	α	β	z	θ
	0	0.13353(6)	0.221(3)	0.43(1)	1.72(2)	0.346(1)
	0.1	0.11898(4)	0.159(4)	0.28(1)	1.59(2)	0.254(2)
	0.3	0.10087(3)	0.159(1)	0.275(3)	1.59(1)	0.251(2)
	0.5	0.08982(4)	0.159(1)	0.275(2)	1.59(1)	0.251(1)

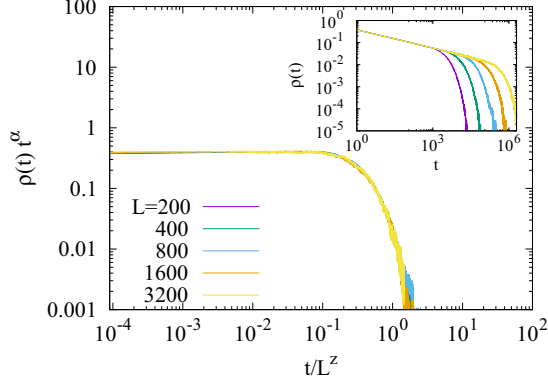


FIG. 4. Numerical estimate of the dynamical exponent z in BARW ($m = 4$) using finite-size scaling. The inset shows the unscaled data of $\rho(t)$ vs t for increasing values of $L = 200, 400, 800, 1600,$ and 3200 as one moves from left to right. In the main panel, log-log plot of $\rho(t)t^\alpha$ vs t/L^z at $p_c = 0.7215$ for $\epsilon = 0$, and all these L values are plotted. A good data collapse is obtained for $z = 1.7$.

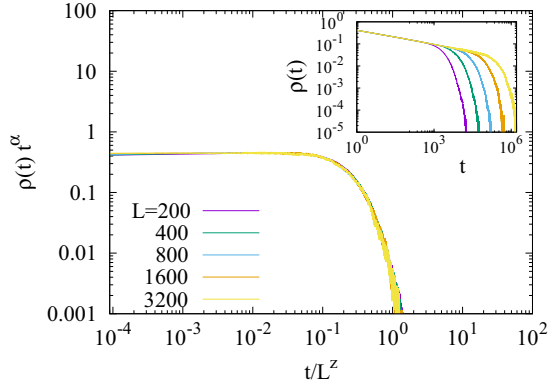


FIG. 5. Numerical estimate of the dynamical exponent z in BARW ($m = 4$) using finite-size scaling. The inset shows the unscaled data of $\rho(t)$ vs t for increasing values of $L = 200, 400, 800, 1600,$ and 3200 as one moves from left to right. In the main panel, log-log plot of $\rho(t)t^\alpha$ vs t/L^z at $p_c = 0.3369$ for $\epsilon = 1/2$, and these L values are plotted. A good data collapse is obtained for $z = 1.74$.

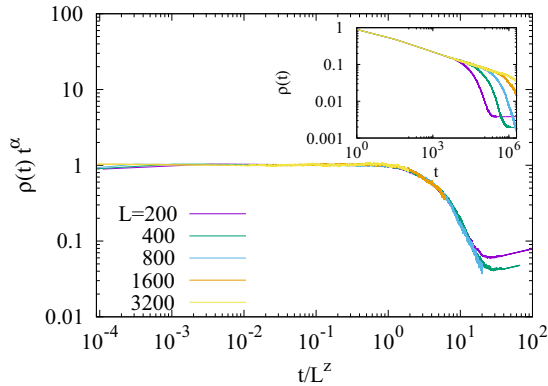


FIG. 6. Numerical estimate of the dynamical exponent z in PCPD using finite-size scaling. The inset shows the unscaled data of $\rho(t)$ vs t for increasing values of $L = 200, 400, 800, 1600,$ and 3200 as one moves from left to right. In the main panel, log-log plot of $\rho(t)t^\alpha$ vs t/L^z at $q_c = 0.13353$ for $\epsilon = 0$, and these L values are plotted. A good data collapse is obtained for $z = 1.72$.

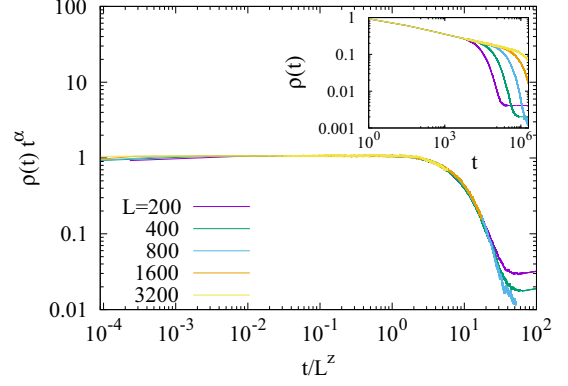


FIG. 7. Numerical estimate of the dynamical exponent z in PCPD using finite-size scaling. The inset shows the unscaled data of $\rho(t)$ vs t for increasing values of $L = 200, 400, 800, 1600,$ and 3200 as one moves from left to right. In the main panel, log-log plot of $\rho(t)t^\alpha$ vs t/L^z at $q_c = 0.08982$ for $\epsilon = 1/2$, and these L values are plotted. A good data collapse is obtained for $z = 1.58$.

We also measure the two-point spatial correlations, $C(r) = \langle s_i(t)s_{i+r}(t) \rangle$, where $\langle \dots \rangle$ is the configuration average. At the critical point, $C(r)$ decays as a power law,

$$C(r) \sim r^{-\theta}, \quad (4)$$

where the exponent $\theta = z\alpha$. In Fig. 10 we plot $C(r)$ versus r in PCPD for $\epsilon = 0$ and $\epsilon = 1/2$, measured at $t = 10^5$. In Table I we put the values of θ obtained from simulations for various values of ϵ . The exponents θ , α , and z seem to satisfy the scaling relation $\theta = z\alpha$ for all ϵ .

IV. RESULTS AND DISCUSSION

In BARW, for $m = 1$ and $\epsilon = 0$, our results match well with the DP exponents obtained previously [14]. For any $\epsilon > 0$, the exponents remain the same as that for $\epsilon = 0$. Therefore, we conclude that the bias does not affect the DP universality class. The BARW model for $m = 4$ belong to the PC class [14] in the absence of any bias ($\epsilon = 0$). Our results indicate the introduction of the bias drastically changes

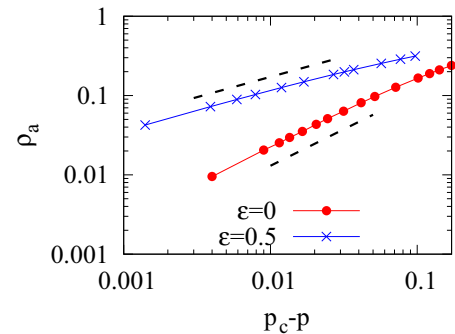


FIG. 8. Log-log plot of ρ_a vs $p_c - p$ in BARW ($m = 4$) for $\epsilon = 0$ and $\epsilon = 1/2$. The slopes of the lines (shown by dashed lines) near $p \rightarrow p_c$ give an estimate of the exponent β . For $\epsilon = 0$, $\beta \sim 0.92$, and for $\epsilon = 1/2$, $\beta \sim 0.51$.

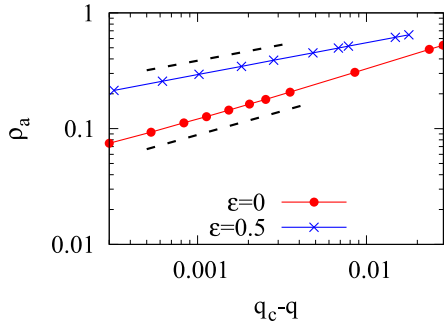


FIG. 9. Log-log plot of ρ_a vs $q_c - q$ in PCPD for $\epsilon = 0$ and $\epsilon = 1/2$. The slopes of the lines (shown by dashed lines) near $q \rightarrow q_c$ give an estimate of the exponent β . For $\epsilon = 0$, $\beta \sim 0.430$, and for $\epsilon = 1/2$, $\beta \sim 0.275$.

the exponents of the PC universality class. This is surprising because the bias does not affect the parity of the system, neither creates any long-range interaction, nor does it give rise to additional conservation laws. It would be interesting to know the universality class that the bias gives rise to for the PC class. We would like to point out that the claim for the existence of a new universality class certainly requires deeper numerical analysis. However, one can check the consistency of the critical exponents via the scaling relations. In Fig. 11 we plot the scaling form:

$$\rho(t, L) \sim L^{-\theta} g(t/L^z), \quad (5)$$

where g is the scaling function. We plot $\rho(t, L)L^\theta$ versus t/L^z for BARW ($m = 4$) when $\epsilon = 0.3$ and find a good data collapse, and the scaling relation $\theta = z\alpha$ is satisfied. Similarly, we have checked that the scaling relation holds good for other ϵ values also.

Our simulations show that the PCPD class crosses over to DP for any nonzero ϵ . A characteristic feature of PCPD is the survival of solitary diffusing walkers for large times. When diffusion of single walkers is blocked in PCPD, its critical behavior is the same as DP [24]. The bias ϵ tends to suppress the diffusion of single walkers away from its parent cluster. For $\epsilon = 1/2$, a single walker cannot leave a cluster and diffuse

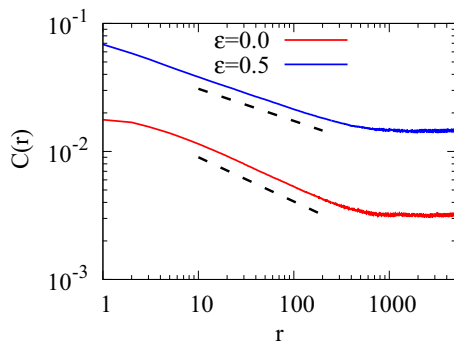


FIG. 10. Two-point correlation function $C(r)$ measured at the critical point q_c in PCPD for $\epsilon = 0$ and $\epsilon = 1/2$ at $t = 10^5$ for a system of size $L = 25 \times 10^3$. The slopes shown by dashed lines give the estimate of θ . For $\epsilon = 0$ (lower line in the panel), $\theta \sim 0.346$ and $\theta \sim 0.251$ for $\epsilon = 1/2$ (upper line).

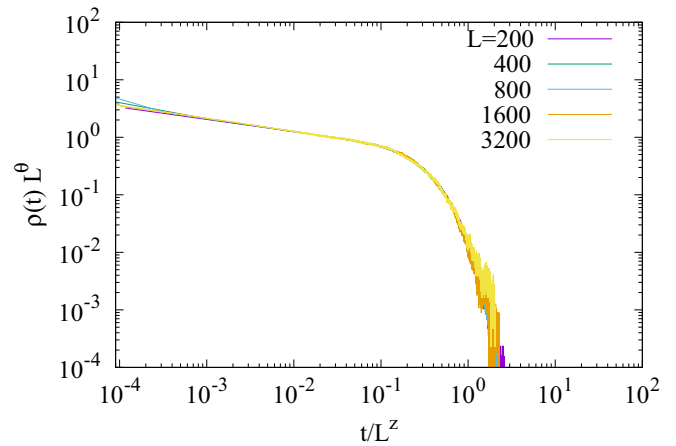


FIG. 11. Numerical estimation of the exponent θ in BARW ($m = 4$) using finite-size scaling and verification of the scaling relation $\theta = z\alpha$: Log-log plot of $\rho(t)L^\theta$ vs t/L^z at $p_c = 0.4182$ when $\epsilon = 0.3$ for $L = 200, 400, 800, 1600$, and 3200 . A good data collapse is obtained for $\theta = z\alpha \sim 0.39$.

as a solitary walker. In Fig. 12 we show the space-time plots for $\epsilon = 0$ and $1/2$ in PCPD at the respective critical points. Clearly, the solitary diffusing walkers do not survive for large times for $\epsilon = 1/2$ as compared to when $\epsilon = 0$. In fact, this effect of solitary diffusing walkers not surviving for large times seems to happen for smaller ϵ values also. This is possibly the reason that for any $\epsilon > 0$, PCPD crosses over to DP.

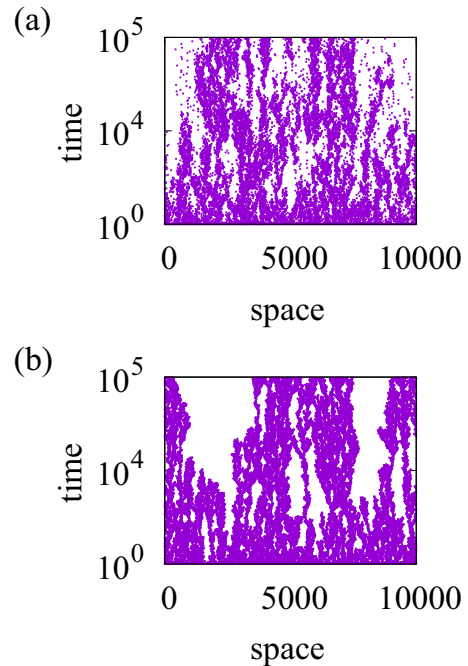


FIG. 12. Space-time plots in PCPD for (a) $\epsilon = 0$ and (b) $\epsilon = 1/2$ at the critical points $q_c = 0.13353$ and 0.08982 respectively. Clearly, the appearance of these plots looks different. This is because, unlike for $\epsilon = 0$, the solitary walkers do not survive for large times when $\epsilon = 1/2$.

We conclude with the following observations. The universality class of DP is robust and remains unaffected by perturbations, which alters the diffusion dynamics as long as the parity symmetry is unaltered. The same cannot be said for the PC and the PCPD universality classes. Parity alone does not guarantee the PC critical behavior, and the PC class may change under perturbations of the diffusion dynamics. However, as long as parity is kept unchanged, PC class does not seem to go to DP class. The PCPD critical behavior is rather

unstable. Although it is not affected by parity, perturbations which arrest the diffusion of single walkers makes it cross over to DP.

ACKNOWLEDGMENTS

B.D. would like to thank G. Ódor and M. A. Muñoz for useful discussions and pointing out important references.

-
- [1] J. Marro and R. Dickman, *Nonequilibrium Phase Transitions in Lattice Models* (Cambridge University, Cambridge, 1999).
 - [2] H. Hinrichsen, *Adv. Phys.* **49**, 815 (2000).
 - [3] G. Ódor, *Rev. Mod. Phys.* **76**, 663 (2004).
 - [4] M. Henkel, H. Hinrichsen, and S. Lübeck, *Non-Equilibrium Phase Transitions* (Springer, Berlin, 2008).
 - [5] D. Mollison, *J. R. Stat. Soc. Ser. B. Methodol.* **39**, 283 (1977).
 - [6] F. Schlögl, *Z. Phys.* **253**, 147 (1972); R. M. Ziff, E. Gulari, and Y. Barshad, *Phys. Rev. Lett.* **56**, 2553 (1986).
 - [7] S. Havlin, and D. ben Avraham, *Adv. Phys.* **36**, 695 (1987).
 - [8] E. V. Albano, *J. Phys. A* **27**, L881 (1994).
 - [9] A. Lipowski and M. Lopata, *Phys. Rev. E* **60**, 1516 (1999).
 - [10] H. Hinrichsen and G. Ódor, *Phys. Rev. E* **60**, 3842 (1999).
 - [11] F. D. A. A. Reis, *Braz. J. Phys.* **33**, 501 (2003).
 - [12] H. Berry, *Phys. Rev. E* **67**, 031907 (2003).
 - [13] H. K. Janssen, *Z. Phys. B* **42**, 151 (1981); P. Grassberger, *ibid.* **47**, 365 (1982).
 - [14] H. Takayasu and A. Y. Tretyakov, *Phys. Rev. Lett.* **68**, 3060 (1992); I. Jensen, *Phys. Rev. E* **47**, R1 (1993); **50**, 3623 (1994); J. Cardy and U. C. Täuber, *Phys. Rev. Lett.* **77**, 4780 (1996).
 - [15] M. J. Howard and U. C. Täuber, *J. Phys. A* **30**, 7721 (1997); G. Ódor, *Phys. Rev. E* **67**, 016111 (2003); For a review, see M. Henkel and H. Hinrichsen, *J. Phys. A* **37**, R117 (2004).
 - [16] I. Dornic, H. Chaté, J. Chave, and H. Hinrichsen, *Phys. Rev. Lett.* **87**, 045701 (2001).
 - [17] S. S. Manna, *J. Phys. A* **24**, L363 (1991).
 - [18] N. Menyhárd, *J. Phys. A* **27**, 6139 (1994).
 - [19] K. Park, H. Hinrichsen, and I.-M. Kim, *Phys. Rev. E* **63**, 065103(R) (2001).
 - [20] S.-C. Park and H. Park, *Phys. Rev. E* **78**, 041128 (2008).
 - [21] S.-C. Park and H. Park, *Phys. Rev. E* **73**, 025105(R) (2006).
 - [22] S.-C. Park and H. Park, *Phys. Rev. E* **79**, 051130 (2009).
 - [23] J. D. Noh and H. Park, *Phys. Rev. E* **69**, 016122 (2004).
 - [24] I. Jensen and R. Dickman, *Phys. Rev. E* **48**, 1710 (1993).
 - [25] M. A. Muñoz, G. Grinstein, R. Dickman, and R. Livi, *Phys. Rev. Lett.* **76**, 451 (1996); M. A. Muñoz, G. Grinstein, and R. Dickman, *J. Stat. Phys.* **91**, 541 (1998).
 - [26] E. V. Albano, *Euro. Phys. Lett.* **34**, 97 (1996).
 - [27] D. Vernon and M. Howard, *Phys. Rev. E* **63**, 041116 (2001).
 - [28] S.-C. Park and H. Park, *Phys. Rev. Lett.* **94**, 065701 (2005).
 - [29] P. Sen and P. Ray, *Phys. Rev. E* **92**, 012109 (2015).